

Efficient charge collection in hybrid polymer/TiO₂ solar cells using poly(ethylenedioxythiophene)/polystyrene sulphonate as hole collector

P. Ravirajan, D. D. C. Bradley, and J. Nelson^{a)}

Department of Physics, Imperial College London, London SW7 2BW, United Kingdom

S. A. Haque and J. R. Durrant

Department of Chemistry, Imperial College London, London SW7 2AZ, United Kingdom

H. J. P. Smit and J. M. Kroon

ECN, Solar Energy, P.O. Box 1, 1755 ZG, Petten, The Netherlands

(Received 21 May 2004; accepted 8 February 2005; published online 28 March 2005)

We report a study of the optimization of power conversion efficiency in hybrid solar cells based on nanostructured titanium dioxide and a poly[2-(2-ethylhexyloxy)-5-methoxy-1,4-phenylenevinylene] (MEH-PPV) based conjugated polymer. Charge collection efficiency is enhanced by introducing a poly(ethylenedioxythiophene)/polystyrene sulphonate (PEDOT) layer (under the gold electrode) as the hole collector. Device performance is maximized for a device with a net active layer thickness of 100 nm. The optimized device has peak external quantum efficiencies $\approx 40\%$ at the polymer's maximum absorption wavelength and yield short circuit current density $\geq 2 \text{ mA cm}^{-2}$ for air mass (AM) 1.5 conditions (100 mW cm^{-2} , 1 sun). The AM 1.5 open circuit voltage for this device is 0.64 V and the fill factor is 0.43, resulting in an overall power conversion efficiency of 0.58%. © 2005 American Institute of Physics. [DOI: 10.1063/1.1890468]

Solar cells based on soluble conjugated polymers are of great interest because of the potential low cost of production by solution processing. Distributed heterojunctions based on blends of polymers with fullerene derivatives are the best studied devices and to date have yielded the highest efficiencies.¹ However, the use of fullerenes as electron acceptors has some disadvantages such as segregation of the components during aging and relatively poor photostability. Metal oxides such as TiO₂,²⁻⁴ ZnO,⁵ and SnO₂ are promising as alternative electron acceptors. They offer good electron transport properties, excellent physical and chemical stability and fabrication via facile techniques. Moreover they offer the possibility of control of the microstructure in order to create a large interfacial area when coated with a polymer film.

Since the first demonstration of working bilayer TiO₂ / polymer devices,² several attempts to increase the charge separation efficiency by increasing the TiO₂ / polymer interfacial area have been reported.^{3,4,6-10} In some early studies,¹² overall device performance was limited by poor penetration of the spin-coated polymer into the porous film, but through a range of strategies this problem is now effectively solved. These strategies include, the use of thin ($\sim 100 \text{ nm}$) nanoporous metal oxide films,^{4,7} melt processing of a polymer possessing a liquid-crystalline phase into porous TiO₂ electrodes,^{3,9} dipcoating the porous TiO₂ electrode in a dilute polymer solution before spin coating a second polymer layer,^{7,10} and the formation of a TiO₂-polymer bulk heterojunction by *in situ* conversion of a titanium isopropoxide precursor codeposited from solution with a conjugated polymer.⁶

Despite the successful interpenetration of polymer and metal oxide components, the highest reported external quantum efficiency (EQE) (25% at 435 nm^2) and power conversion efficiencies for TiO₂ / polymer hybrids ($< 0.2\%$ under 1

sun⁴) are still low compared to the best values for other polymer-based solar cells. Performance is typically limited by low external quantum efficiency, which leads to low short circuit current densities^{3,4,6-9} of only a few hundreds of $\mu\text{A cm}^{-2}$ compared to over 5 mA cm^{-2} for polymer-fullerene devices made from similar polymers. The low short circuit current density may be attributed to low interfacial area, short exciton diffusion lengths for the polymer compared to the pore size of the nanostructured film, poor polymer hole mobility, or fast interfacial recombination. In a separate study of the relationship between polymer optoelectronic properties and device performance,¹⁰ we have found that the factors in an optimized device structure with greatest influence on device efficiency are the polymer exciton diffusion length and absorption range, followed by the hole mobility.

In this letter we report the optimization of the device structure for a hybrid MEH-PPV polymer /TiO₂ photovoltaic (PV) device. We focus on a system consisting of the copolymer, poly{[1, 4-phenylene-(4-methylphenyl)amino-4, 4'-diphenylene-(4-methylphenyl)amino-1, 4-phenylene-ethynylene-2-methoxy-5-(2-ethylhexyloxy)-1, -phenylene-ethynylene]-co-(2, 5-dimethoxy-1, 4-phenylene-ethynylene-2-methoxy-5-(2-ethylhexyloxy)-1, 4-phenylene-ethynylene)} (TPD(4M)-MEH-M3EH-PPV)¹⁰ and nanocrystalline porous TiO₂. TPD(4M)-MEH-M3EH-PPV was selected for its high hole mobility ($\sim 3 \times 10^{-4} \text{ cm}^{-2} \text{ V}^{-1} \text{ s}^{-1}$ at $2.5 \times 10^5 \text{ V/cm}$), visible absorption range (300–525 nm), ability to sensitize TiO₂ (possibly assisted by the alkoxy side chain oxygen atoms), relatively long exciton diffusion length ($\sim 15 \text{ nm}$) and moderate ionization potential (5.3 eV).¹⁰ This combination of properties was shown in Ref. 10 to lead to the best performance from among a group of similar polymers.

The devices were fabricated as described in Ref. 10. Six devices were fabricated per substrate to check reproducibility. Each device (area= 4.2 mm^2) consists of four layers on top of the indium tin oxide (ITO) substrate, namely a dense

^{a)}Electronic mail: jenny.nelson@imperial.ac.uk

TiO₂ hole blocking layer (HBL), a porous nanocrystalline TiO₂ layer, a dip-coated polymer layer, and a spin-coated polymer layer. It is important to note that the polarity of the device is the reverse of most organic PV devices, such that electrons, not holes, travel towards the ITO. Because of the high temperature processing of the TiO₂ films, it is necessary that the TiO₂ is deposited on the ITO before the organic layers, and this requires that the ITO acts as the electron collecting electrode, and the top contact as the hole collector. The thicknesses of the layers in each device were (unless stated otherwise) as follows: HBL (~40 nm), porous TiO₂ (~100 nm), dip and spin coated polymer (~50 nm combined), PEDOT (~50 nm), and Au (~70 nm). The HBL is required to prevent shunt paths between the polymer and the ITO substrate. The porous TiO₂ layer is required to increase the interfacial area for charge separation, as shown in Ref. 7. The dip coating step improves both the sensitization of the TiO₂ film compared to spin coating alone and the fill factor of the TiO₂ / polymer device leading to an increase of 50% in the overall power conversion efficiency. The final, spin coated polymer layer is required to fill the pores, thus increasing optical density and improving film uniformity.⁷

For porous TiO₂ film deposition, colloidal TiO₂ (~20 nm diameter) paste synthesized as described in Ref. 11 was dissolved in tetrahydrofuran (THF) (10 mg/ml) and deposited by spin coating followed by sintering at 450 °C. In some devices, a layer of PEDOT:PSS (BAYTRON P, HC Stark, standard grade) in aqueous dispersion was deposited on top of the polymer layer before depositing the metal contact. In order to improve the wetting of the polymer by the PEDOT:PSS, the PEDOT solution was first ultrasonicated for 15 min and then heated for 15 min at 90 °C, filtered with a 0.45 μm filter and spin coated on the dried semiconducting polymer layer in a water free environment. The sample was then annealed at 100 °C for 5 min under N₂ gas. *J-V* and quantum efficiency measurements were made in air as described in Ref. 7. Photoinduced charge transfer yield and recombination kinetics were measured on ITO / HBL / porous TiO₂ / polymer samples (without PEDOT and Au) using nanosecond–millisecond transient optical spectroscopy as described in Ref. 10. Such measurements of the photoinduced charge transfer yield confirm that polymer infiltration into the porous TiO₂ is excellent.¹⁰

Figure 1 shows *J-V* characteristics of two devices prepared as described above with and without the PEDOT layer under AM1.5 equivalent illumination (100 mW cm⁻²). The inset shows the corresponding dark *J-V* characteristics of the cells. The PEDOT layer increases the short circuit current density (*J*_{SC}) from 0.6 to 1.6 mA cm⁻². The open circuit voltage (*V*_{OC}), however, slightly decreases by about 0.1 V. The overall efficiency is approximately doubled (from η = 0.23% to 0.43%). Although PEDOT is well known to improve the performance of organic PV devices, it has normally been used in the conventional polarity where PEDOT is deposited on to ITO and the ITO acts as hole collector.

There are several possible reasons for the improvement in *J*_{SC} resulting from insertion of the PEDOT layer. One explanation is that PEDOT may cause a chemical doping of the polymer that reduces the contact resistance between the polymer and metal contact. A second possibility is that the PEDOT layer may protect the polymer film from damage during evaporation of the Au electrode,¹² which could lead to an increase in the series resistance of the device. A third

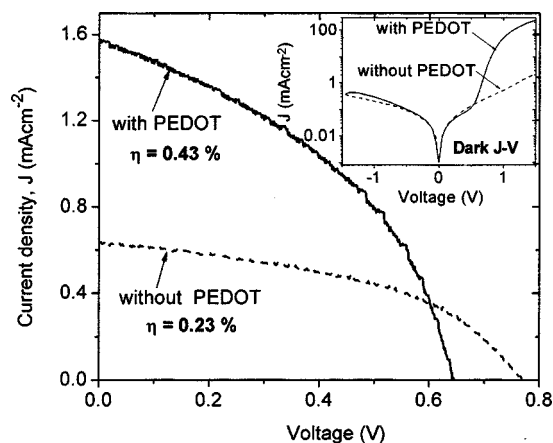


FIG. 1. *J-V* characteristics, under AM 1.5 solar spectrum irradiation (100 mW cm⁻², 1 sun), of multilayer devices (ITO / HBL / porous TiO₂ (120 nm) / TPD(4M)-MEH-M3EH-PPV(50 nm) / PEDOT(*X*nm) / Au) with (*X* = 50 nm) or without (*X* = 0 nm) the PEDOT layer. The inset shows the dark *J-V* characteristics of the multilayer device with PEDOT (solid line) and without (dash line).

possibility is that PEDOT improves collection by minimizing the energy step between polymer and top contact. Experimental⁷ and simulation¹⁵ studies show that interfacial energy steps should be minimized for efficient charge transfer between active layers and electrodes. It has been shown that the work function of Au on top of conjugated polymers may be smaller than the expected value of 5.1 eV by 0.2–0.3 eV.¹⁴ Since the ionization potential of TPD(4M)-MEH-M3EH-PPV polymer is 5.3 eV,¹⁰ the energy step at the polymer / Au interface is expected to be at least 0.4 eV in the device without the PEDOT layer. In contrast, for the device with the PEDOT layer there should be no interfacial energy step because the PEDOT work function of 5.2–5.3 eV is similar to the ionization potential of the polymer.¹⁰ The inset to Fig. 1 shows that the forward-bias dark current for the device with PEDOT is much higher (100 times at +1.5 V) than for the device without PEDOT, confirming that the energy barrier for hole injection at the polymer / metal interface is reduced by introduction of the PEDOT layer. The decrease in *V*_{OC} upon introduction of the PEDOT layer is also quite consistent with a reduced interfacial energy step and increased hole injection. Note that the effect on *V*_{OC} is the reverse of that expected, if *V*_{OC} was controlled by the difference in electrode work functions.

In order to optimize the device structure, we varied the thickness of the active layers. The inset to Fig. 2(a) shows the AM 1.5 power conversion efficiencies for devices with different porous TiO₂ layer thicknesses, from 100 to 500 nm for a fixed semiconducting polymer thickness of 100 nm. The efficiency is maximum when the ratio of the porous TiO₂ layer thickness to the effective polymer layer thickness is about 2:1. This result is reasonable, since there should be just enough polymer to fill the pores at this ratio, assuming that the porosity of the TiO₂ films is about 50%. Next, keeping the optimum ratio of 2:1 for the porous TiO₂ and semiconducting polymer layer thicknesses the effect of total device thickness was studied. Figure 2(a) compares the *J-V* characteristics for thick (200 nm porous TiO₂, 100 nm polymer) and thin (100 nm porous TiO₂, 50 nm polymer) devices under AM 1.5 conditions. The thin device shows an open circuit voltage *V*_{OC} = 0.64 V, a short circuit current density *J*_{SC} = 2.1 mA cm⁻² and a fill factor of 0.43. Its resulting AM

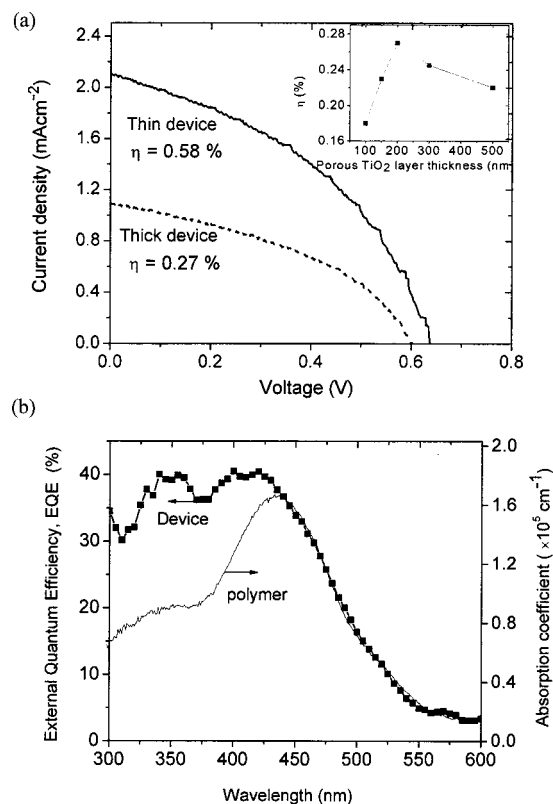


FIG. 2. (a) J - V characteristics under A. M. 1.5 conditions (1 sun) for both thick (200 nm porous TiO₂, 100 nm polymer) and thin (100 nm porous TiO₂, 50 nm polymer) devices. The inset shows the AM 1.5 power conversion efficiency for devices with different porous layer thicknesses for a constant polymer thickness (100 nm); (b) EQE spectrum of the thin multilayer device (filled squares) and the corresponding absorption spectrum of the polymer (solid line).

1.5 power conversion efficiency, 0.58%, is more than twice that of the thick device, namely 0.27%. The higher efficiency may be attributed to a reduced series resistance for the thinner TiO₂ and polymer layers, and to improved charge collection efficiency. Attempts to increase device efficiency further by reducing the active layer thickness were not successful. However, very thin devices are subject to high roughness and shunt losses, which tend to degrade performance and mask any effect of thickness. Both J_{SC} and η show linear dependence on light intensity up to 100 mW cm⁻². This indicates that bimolecular recombination is minimal compared to charge collection.

Figure 2(b) shows the external quantum efficiency spectrum of the thin device together with the absorption spectrum of the semiconducting polymer. The device shows a maximum EQE of 40% at the maximum absorption of the polymer. This is almost two times higher than the highest EQE previously reported for polymer/TiO₂ devices³ and is comparable with EQEs reported for the best solid state dye sensitised¹⁵ and small-molecule¹⁶ solar cells. The high EQE suggests that high photocurrents and efficiencies can be achieved for polymer/TiO₂ devices given polymers with a suitable absorption range. Integrating the product of the measured EQE with the photon flux density of the AM1.5 solar spectrum yields a short circuit current density of about 2.5 mA cm⁻², which is consistent with the measured J_{SC} un-

TABLE I. Comparison of the performance (AM 1.5) of our devices with that of the best previously reported hybrid TiO₂ / polymer solar cells.

Polymer	J_{SC} (mA cm ⁻²)	V_{OC} (V)	FF	η (%)	Reference
F8T2	0.40	0.94	0.44	0.17	7
MEH-PPV	0.40	1.10	0.42	0.18	4
MDMO-PPV	0.60	0.51	0.42	0.19^a	6
TPD(4M)-MEH-M3EH-PPV	2.10	0.64	0.43	0.58	This work

^aPerformance under 70 mW cm⁻², while others under 100 mW cm⁻².

der AM1.5 conditions of 2.1 mA cm⁻². Table I compares the performance characteristics of our devices with the best previously reported hybrid TiO₂ / polymer solar cells under AM1.5 illumination. The better performance of our device can be attributed to improvements in device design, polymer pore penetration, and the specific properties of the polymer, including its hole mobility and ability to sensitize TiO₂.

In conclusion, we have reported high efficiency multilayer hybrid TiO₂ / polymer solar cells based on nanocrystalline TiO₂ and a TPD containing MEH-PPV polymer. We observe strong effects both from introduction of a PEDOT layer and from optimizing the active layer thickness on the photovoltaic performance of the device.

The authors thank Professor H. H. Hörhold for providing the TPD(4M)-MEH-M3EHPPV polymer and the Commission of the European Community (Project MOLYCELL Contract No. 502783), and the ECN-ENGINE Program for financial support. P.R. thanks the Commonwealth Universities for a Scholarship.

¹F. Padinger, R. S. Rittberger, and N. S. Sariciftci, *Adv. Funct. Mater.* **13**, 85 (2003).

²A. C. Arango, L. R. Johnson, V. N. Bliznyuk, Z. Schlesinger, S. A. Carter, and H. H. Horhold, *Adv. Mater. (Weinheim, Ger.)* **12**, 1689 (2000).

³K. M. Coakley and M. D. McGehee, *Appl. Phys. Lett.* **83**, 3380 (2003).

⁴A. J. Breeze, Z. Schlesinger, S. A. Carter, and P. J. Brock, *Phys. Rev. B* **64**, 125205 (2001).

⁵W. J. E. Beek, M. M. Wienk, and R. A. J. Janssen, *Adv. Mater. (Weinheim, Ger.)* **16**, 1009 (2004).

⁶P. A. van Hal, M. M. Wienk, J. M. Kroon, W. J. H. Verhees, L. H. Slooff, W. J. H. van Gennip, P. Jonkheijm, and R. A. J. Janssen, *Adv. Mater. (Weinheim, Ger.)* **15**, 118 (2003).

⁷P. Ravirajan, S. A. Haque, J. R. Durrant, D. Poplavskyy, D. D. C. Bradley, and J. Nelson, *J. Appl. Phys.* **95**, 1473 (2004).

⁸A. C. Arango, S. A. Carter, and P. J. Brock, *Appl. Phys. Lett.* **74**, 1698 (1999).

⁹K. M. Coakley, Y. X. Liu, M. D. McGehee, K. L. Frindell, and G. D. Stucky, *Adv. Funct. Mater.* **13**, 301 (2003).

¹⁰P. Ravirajan, S. A. Haque, J. R. Durrant, D. D. C. Bradley, and J. Nelson, *Adv. Funct. Mater.* (in press).

¹¹M. Spath, P. M. Sommeling, J. A. M. van Roosmalen, H. J. P. Smit, N. P. G. van der Burg, D. R. Mahieu, N. J. Bakker, and J. M. Kroon, *Prog. Photovoltaics* **11**, 207 (2003).

¹²A. Ioannidis, J. S. Facci, and M. A. Abkowitz, *J. Appl. Phys.* **84**, 1439 (1998).

¹³J. Nelson, J. Kirkpatrick, and P. Ravirajan, *Phys. Rev. B* **69**, 035337 (2004).

¹⁴G. G. Malliaras, J. R. Salem, P. J. Brock, and C. Scott, *Phys. Rev. B* **58**, 13411 (1998); A. J. Campbell, D. D. C. Bradley, and H. Antoniadis, *J. Appl. Phys.* **89**, 3343 (2001).

¹⁵J. Kruger, R. Plass, L. Cevey, M. Piccirelli, M. Gratzel, and U. Bach, *Appl. Phys. Lett.* **79**, 2085 (2001).

¹⁶P. Peumans and S. R. Forrest, *Appl. Phys. Lett.* **79**, 126 (2001).